Int. J. Electrochem. Sci., 14 **(2019)** 8793 – 8804, doi: 10.20964/2019.09.34

International Journal of
ELECTROCHEMICAL
SCIENCE
www.electrochemsci.org

Mesoporous biochar derived from silkworm excrement for high-performance supercapacitors

Xiaozhan Zhang[1], *Zhenyu Wang*[1], *Guoju Dang* [1], *Daoming Zhang*[1], *Dunfan Zhou*[1], *Yaping Fan*[1], *Meng Yu*[1], *Quansheng Zhang*[1,*], *Jingying Xie*[2,*]

[1] School of Chemical and Environmental Engineering, Shanghai Institute of Technology, Shanghai 201418, China.
[2] Shanghai Institute of Space Power Sources, Shanghai 200245, China.
[*]E-mail: zhangquansheng@sit.edu.cn .

Received: 24 April 2019 / *Accepted:* 27 June 2019 / *Published:* 31 July 2019

In this work, Preparation of mesoporous carbon materials (Original-SE) by high temperature carbonization of biomass materials derived from silkworm has been successfully fabricated as high-performance and wide potential window electrodes for supercapacitors. pickling mesoporous carbon materials (Pickling-SE) are obtained from mesoporous carbon materials (Original-SE) via chemical (HCL) method. It is interesting that the pickling mesoporous carbon materials possesses a higher specific surface area of 293.97 m^2/g than that of 112.64 m^2/g for mesoporous carbon materials. A more excellent electrochemical performance of a specific capacitance of 291.5 F/g for Pickling-SE electrodes than that 208.3 F/g for Original-SE electrodes at 1A/g in 1M Li_2SO_4 electrolyte, and a higher stability for Pickling-SE electrodes (97.2%) than Original-SE electrodes (91.1%) over 5000 cycles.

Keywords: supercapacitors, silkworm excrement, Mesoporous, higher specific surface

1. INTRODUCTION

The modern archaeological proofs that our country is the first country to start of mulberry sericulture [1]. In neolithic age, it has been 5000 years of history that our ancestors planted mulberry and raised silkworm, which has deep cultural heritage [2]. In China, silkworm excrement is a traditional Chinese medicine and stems from most of the active ingredients which consist of the consumption of mulberry leaf protein, carbohydrates and fatty substances, after silkworm eating mulberry leaves [3]. Silkworm excrement is one of the largest byproducts in sericulture production with an annual output of more than 5 million tons. And it is a cheap and abundant silkworm resource [4]. The current popular

research on silkworm excrement is used for concentrate feed of livestock and poultry, fertilizer, medicine and chemical raw materials (chlorophyll, leaf protein, carotenoids, pectin, etc.) [5,6,7].

At the same time, silkworm excrement is a kind of biological carbon source, also can be used as a kind of material preparing of graphene [8]. It is not only cheap, environmentally friendly, stable, silkworm excrements, containing a number of inorganic salts, chitosan, also can stabilize structure and enhance surface area during preparing for carbon materials [9,10]. carbon materials have the advantages of excellent electrical properties, good cycle stability, and high specific surface area, and are therefore one of the most commonly used electrode materials [11-15]. In recent years, due to the shortage of fossil resources, the application and development of carbon materials have been restricted. The preparation of carbon materials from renewable biomass resources has always been the focus of researchers [16-22].

In this work, we have further studied the mesoporous carbon derived from biomass materials of silkworm excrement for supercapacitor electrodes, we have used cyclic voltammetry and chronopotentiometry in a half cell and in a single cell without introducing any binder. Mesoporous carbon materials (Original-SE) electrodes exhibits lower capacitance to those of pickling mesoporous carbon materials (Pickling-SE) electrodes under similar conditions. We have attributed this remarkable capacitance increase to the increase of mesoporous. It is expected that pickling mesoporous carbon materials for supercapacitors will be able to meet the cost and performance specifications required for the widespread use of supercapacitors.

2. EXPERIMENT

2.1. Preparation of biochar

The silkworm excrements were supplied from autotrophic of silkworm, dried in the sun and kept in the dry place. The dry material was ground and sieved by 100 meshes. Then the material was carbonized at 700℃ for 10h in furnace in N_2 atmosphere (the temperature ramping rate was 5℃/min) and then natural cooling to room temperature (Denoted as Original-SE), the collected material was sieved to remove inorganic salts and impurities by hydrochloric acid (HCL) pickling (Denoted as Pickling-SE) [23-25].

2.2. Preparation of electrodes

The working electrodes were prepared by mixing active materials (Carbonized Silkworm excrement), acetylene black and Polytetrafluoroethylene (PTFE were dissolved in ultrapure water at a percent of sixty) in a mass ratio of 8:1:1 to obtain a slurry. Full mixing, rolling into pieces, the poles are round, the diameter are 5mm, the thickness are about 0.025mm. The collector of the test electrode is a round glass carbon electrode, which is placed directly on the surface of the glass carbon electrode and is fixed by the filter cloth.

2.3. Materials characterization

The mesoporous carbon materials and hydrochloric acid pickling mesoporous carbon material were characterized by scanning electron microscope (SEM, S-3400N, Hitachi), transmission electron microscope (TEM) and high resolution transmission electron microscope (HRTEM) from JEOL JEM-2100F, operated at accelerating voltage of 200 kV. The crystal structures of the carbon materials were determined by X-ray diffraction (XRD) in the D8 Advance X-ray diffractometer (German Bruker AXS) equipped with graphite monochromator and Cu target (λ≈0.15406 nm) at scanning rate of 5℃/min using accelerating voltage of 40 kV and emission current of 40 mA. X−ray photoelectron spectroscopy (XPS) measurements were carried out using a spectrometer with Al Kα radiation (Thermo Scientific Escalab 250Xi). The surface areas were tested by nitrogen adsorption/desorption analysis with a Quantachrome Instruments (Micromeritics ASAP 2020 HD88).

2.4. Electrochemical measurement

Electrochemical testing was performed using a CHI760D electrochemical workstation in a three-electrode system using platinum wire as the counter electrode and Ag/AgCl electrode as the reference electrode. For Cyclic voltammetry (CV) and constant current charge/discharge, a solution of 1mol/L NaOH ,1mol/L Li_2SO_4 were used as the test solution, respectively.

3. RESULTS AND DISCUSSION

3.1. Materials(SE) characterization

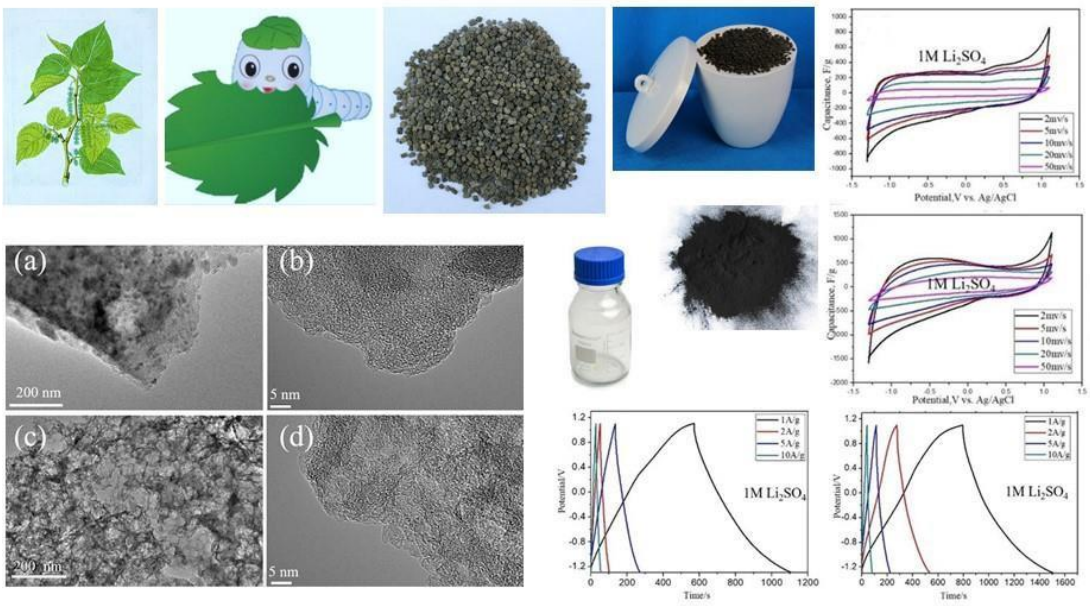

Figure 1. Overall outline of the study.

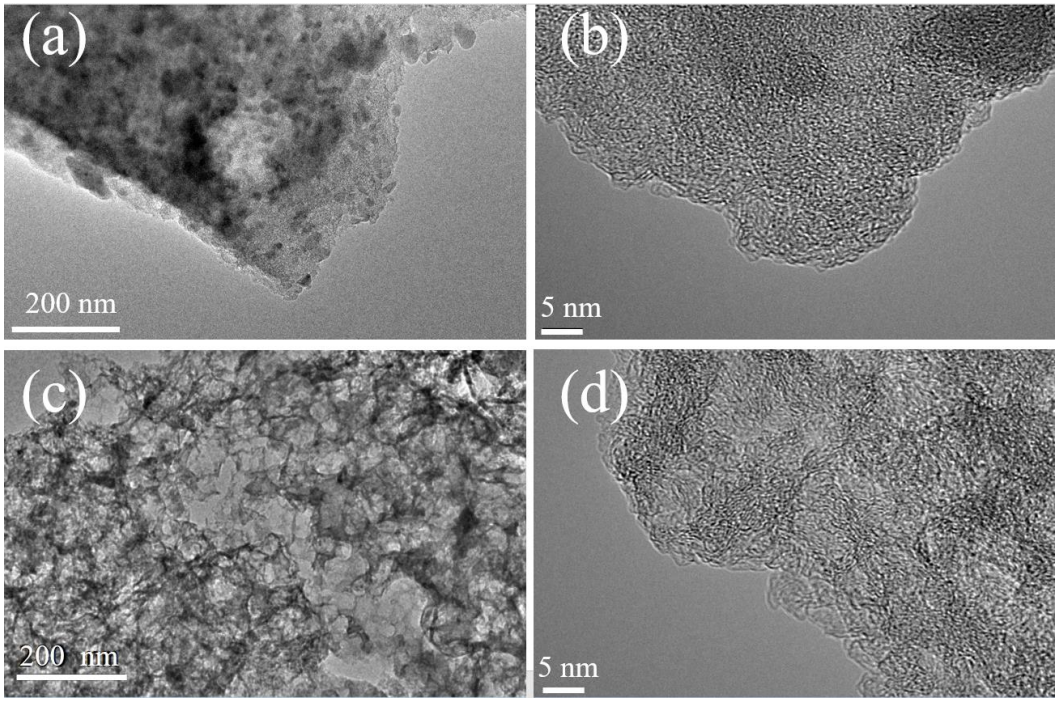

Figure 2. (a) Low-and (b) high-magnification TEM images of Original-SE sample. (c) Low- and (d) high-magnification TEM images of Pickling-SE sample.

Figure 2 presents the TEM images of the Original-SE and Pickling-SE samples, the effect of pickling on the samples is fully demonstrated by TEM images (Figure 1c). The obvious changes of morphology could be clearly observed after the impurities and pickling by hydrochloric acid as compared in Figure 1a and 1c. Pickling-SE samples (Figure 1c and 1d) show much richer porosity than that of Original-SE samples (Figure 1a and 1b), Figure 1c displays a unique hierarchical porous structure with a 3D interconnected porous network reveals abundant micropores and the holes are homogeneously dispersive [16]. The amorphous micropores formed during the pickling process, and the irregular particles rich in micropores can provide a large adsorption interface for the electrolyte ions, which is beneficial to the performance of the supercapacitors [17].

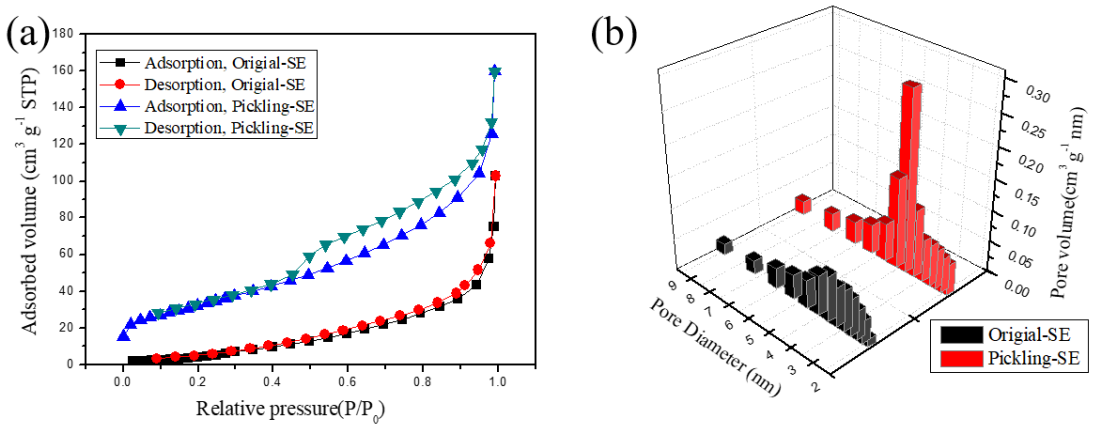

Figure 3. BET characterization, (a) nitrogen adsorption−desorption isotherms and (b) the corresponding pore size distribution curves for Original-SE sample and Pickling-SE sample, respectively.

The Original-SE and Pickling-SE samples were studied by the BET method. The comparison of N2 adsorption/desorption isotherms (Figure 3a) and pore size distribution curves (Figure 3b) of the samples were depicted in Figure 3. As can be seen, the less similarity of their isotherms indicates that N2 adsorption and desorption on the samples may follow different kinetics. The isotherm of Pickling-SE samples is a typical type-IV isotherm with the type H4 hysteresis loop, indicating the existence of a large amount of mesoporous in Pickling-SE samples [26]. The closely vertical tail at high relative pressure (0.9-1.0) indicates that macropores exist in Pickling-SE samples [16,27,28]. This suggests that the Pickling-SE samples has a higher percentage of mesoporous structures than the Original-SE samples. The values of BET specific surface area are 112.64 and 273.97 m2/g for Original-SE and Pickling-SE samples, respectively. As shown in Figure 3b, the distribution of mesoporous of the Pickling-SE sample noticeably increase in the range of 2-6nm. These changes clearly indicate that the pickling increases the specific surface area and number of mesoporous.

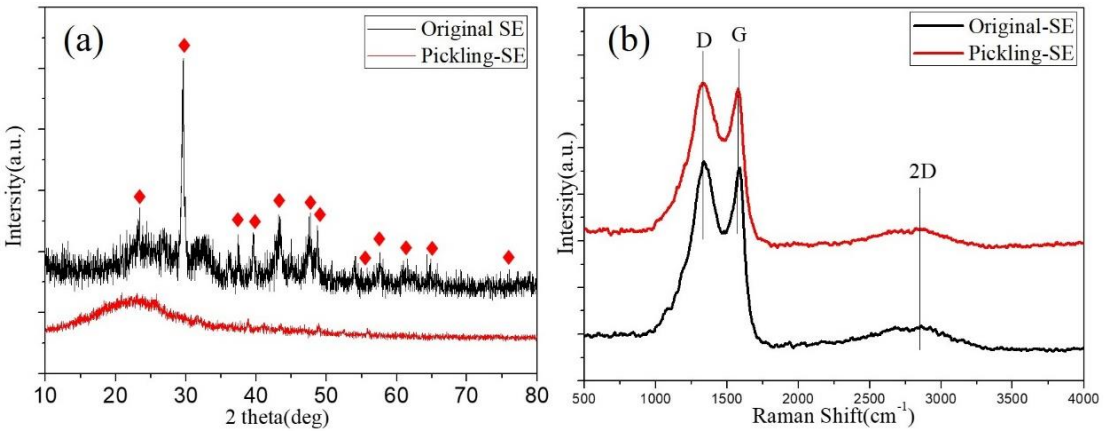

Figure 4. (a) Powder X-ray diffraction patterns of Original-SE sample (black line) and Pickling-SE sample (red line), respectively. (b) Raman spectra of Original-SE sample (black line) and Pickling-SE sample (red line), respectively.

The crystalline properties of SE were also characterized by X-ray diffraction. Figure 4a clearly shows that the diffraction peaks of cellulose crystals were observed in both cases. It is observed that an effective disappear of the sharp and narrow peaks compared to the diffraction peaks of the Original-SE samples. All the reflection peaks of the Original-SE sample (black line) could be indexed to hexagonal $CaCO_3$, the typical diffraction peaks at $2\theta=29.5^{\circ}$ are associated with the (114) facet, and the XRD patterns are in accordance with the literature values (JCPDS file Card No.47-1743), this character is presented in case of the folium mori, which is the food for silkworm consist of vast CaC_2O_4 [29,30]. The hump in the range 20-30° implies the high degree of disorder expected for the produced carbonaceous material. No sharp peaks appeared in the patterns, indicated that Pickling-SE was amorphous [18,20].

Raman spectroscopy was carried out to analyze the carbon structure (Figure4b). Three characteristic peaks located at ~1348 cm^{-1}, 1590 cm^{-1} and 2800 cm^{-1} are observed, Both the D-peak and the G-peak are Raman characteristic peaks of C atom crystals, which are near 1300cm^{-1} and 1580cm^{-1}, respectively. The D-peak represents the defect of the C atomic lattice, and the G-peak represents In-

plane stretching vibration of C atom sp^2 hybridization. I_D /I_G is the intensity ratio of D-peak and G-peak. This ratio can be used to describe the intensity relationship of these two peaks. The larger the value, the more defects of C-crystals [31-33]. The intensity ratio of the signals I_D /I_G was 0.95, which was smaller than 1, indicating high graphitization degree was obtained. Good graphitization means good electrical conductivity and good power density [34-36].

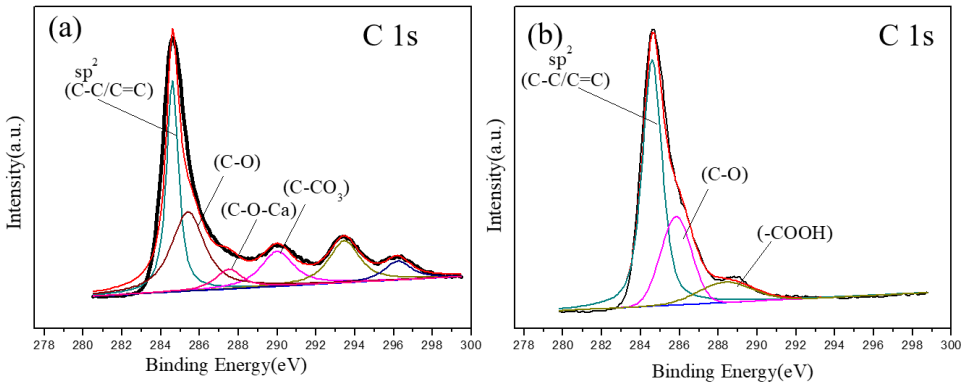

Figure 5. High-resolution X-ray photoelectron spectroscopy scans of C 1s. (a) Original- SE samples. (b) Pickling-SE samples.

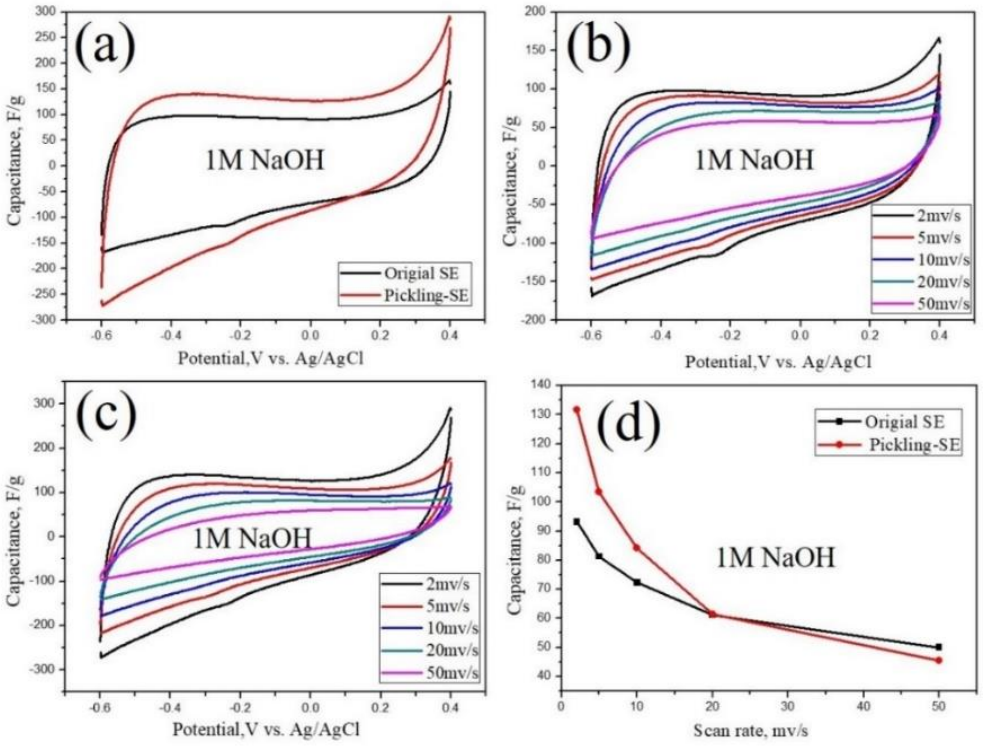

Figure 6. CV curves (a) Comparison of Original-SE electrode and Pickling-SE electrode at 2mV/s in 1M NaOH electrolyte (b) Original-SE electrodes (c) Pickling-SE electrode at different scanning rate ranging from 2 to 50 mV/s in 1M NaOH electrolyte. (d)The specific capacitance comparisons of Original-SE electrodes (black line) and Pickling-SE electrodes (red line) under different scanning rates.

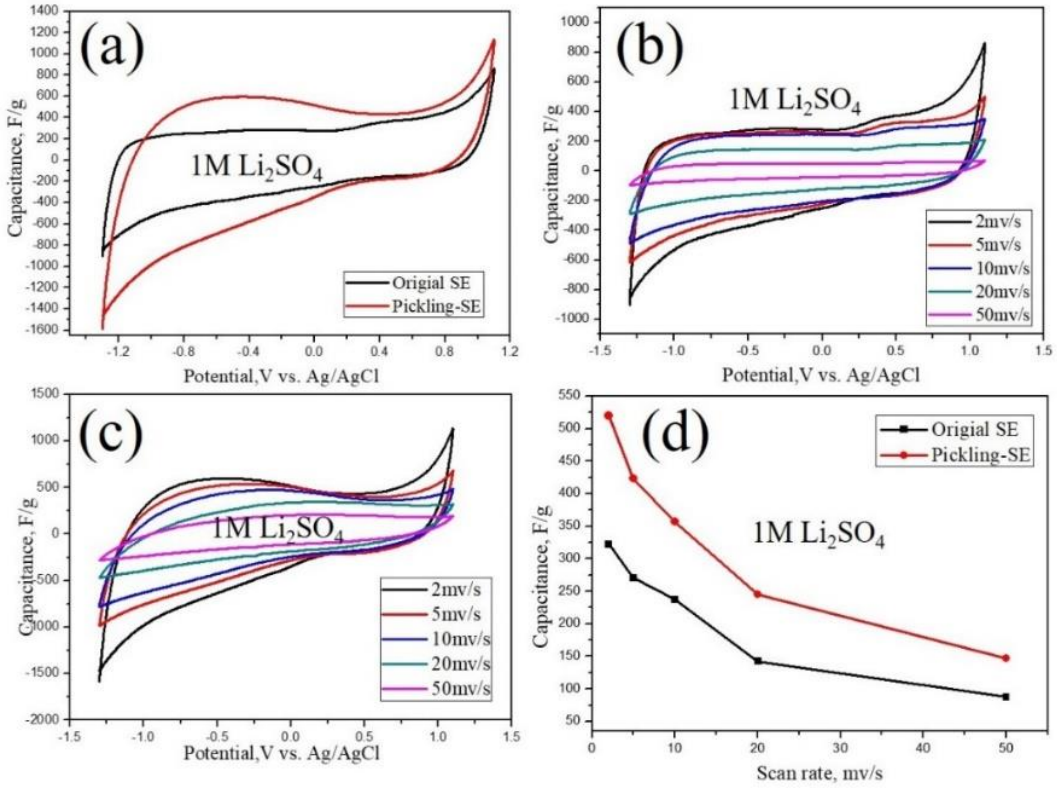

Figure 7. CV curves (a) Comparison of Original-SE electrode and Pickling-SE electrode at 2mV/s in 1M Li_2SO_4 electrolyte (b) Original-SE electrodes (c) Pickling-SE electrode at different scanning rate ranging from 2 to 50mV/s in 1M Li_2SO_4 electrolyte. (d)The specific capacitance comparisons of Original-SE electrodes (black line) and Pickling-SE electrodes (red line) under different scanning rates.

The X-ray photoelectron spectroscopy (XPS) measurements are carried out for the surface chemical structures of the SE samples. The high-resolution XPS C 1s scan of Original-SE samples shows that C consists primarily of sp^2 -hybridized carbon, along with some C−C, C=C, C−O, C−O−Ca, C−CO_3 and -COOH moieties (Figure 5a). In addition, the C−O−Ca and C−CO_3 moieties are not found in Figure 5b, the high- resolution XPS C 1s spectrum of Pickling-SE sample.

Analysis of electromechanical materials by cyclic voltammetry. Figure 6a shows the CV curves of the comparison of Original-SE electrode and Pickling-SE electrode at 2mV/s in 1M NaOH electrolyte, and the potential windows conformably are -0.6 - 0.4V. All cyclic voltammetry curves showed relatively good rectangular shapes in their CV curves, representing their good capacitive behavior [25]. All cyclic voltammetry curves appear similar to holding shapes without other impurity peaks, indicating an ideal double layer capacitor instead of a Faraday tantalum capacitor [28]. As expected, the specific capacitances of Original-SE electrodes (93.2F/g) are lower than that of Pickling-SE electrodes (131.5 F/g) at 2 mV/s. CVs of various scan rates in 1 M NaOH electrolyte are presented in Figure 6b and 6c, respectively. And the electrodes retain their high capacitance values and rectangular shape. In addition, the electrodes behave the same performance of larger capacitance in Li_2SO_4 electrolyte as shown in Figure 7a, the specific capacitances of Original-SE electrode and Pickling-SE electrode are 312.8 F/g and 519.58 F/g

at 2 mV/s, respectively. The above results are the higher capacitance of Pickling-SE electrodes can be attributed to its larger surface area and mesoporous structure. Large surface area and good stratified pore distribution for electrolytes Diffusion, thus ensuring that the electrode has good conditions under large magnification conditions Capacitance characteristics. CVs of various scan rates in 1 M Li_2SO_4 electrolyte are presented in Figure 7b and 7c, respectively. As is shown, impressive potential windows of 2.4 V for SE electrodes in 1 M Li_2SO_4 electrolyte can be obtained

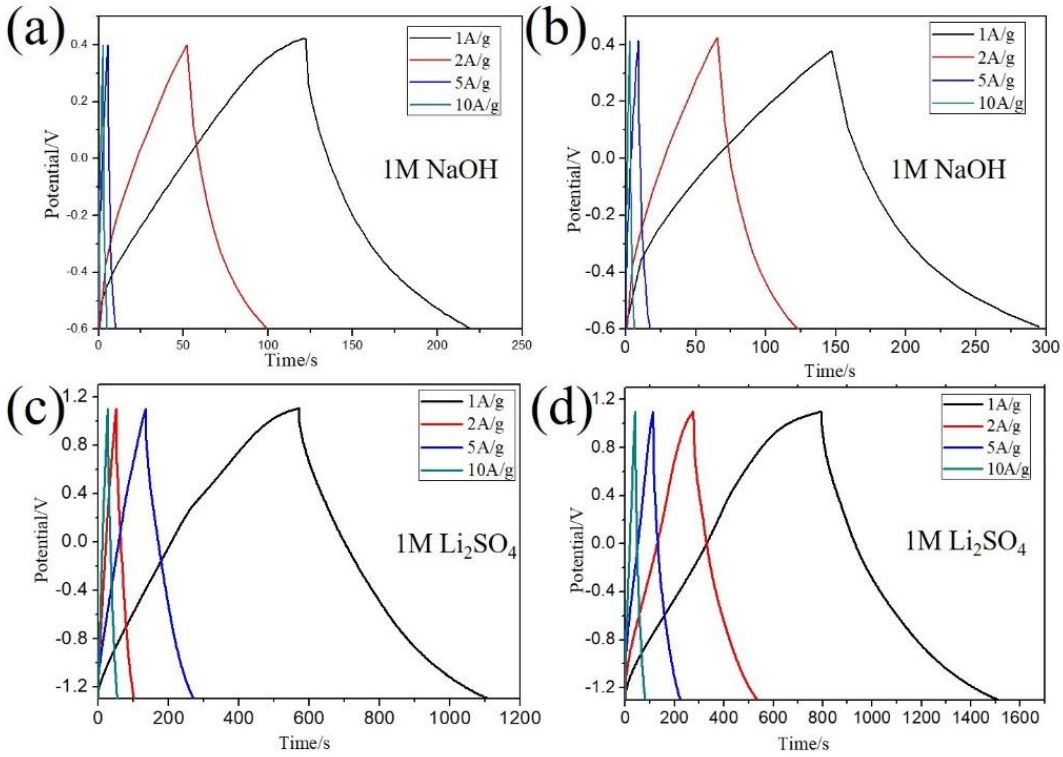

Figure 8. Galvanostatic charge/discharge curves at different current density for (a)Original-SE electrodes in 1M NaOH electrolyte (b)Pickling-SE electrodes 1M NaOH electrolyte (c) Original-SE electrodes in 1M Li_2SO_4 electrolyte and (d) Pickling-SE electrodes 1M Li_2SO_4 electrolyte.

The specific capacitance Cs (F g^{-1}) of constant current charge/discharge has been calculated based on the following equation:

$Cs(F\ g^{-1})=I\Delta t/m\Delta V$

Where I (mA) is the charge and discharge current, Δt(s) is the time of discharge, m (mg) is the weight of the active material, and ΔV (V) is the voltage interval.

It can be seen from the figures that the activated silkworm excrement exhibit the characteristics of typical electric double layer capacitor with an isosceles triangle. The symmetrical shape of the GCD curves suggests the high reversibility of the electrodes [25]. As expected, the specific capacitances of Original-SE electrodes (95.6F/g) are lower than that of Pickling-SE electrodes (150.3 F/g) at 1A/g. GCDs of various Current density in 1 M NaOH electrolyte are presented in Figure 8a and 8b,

respectively. the specific capacitances of Original-SE electrodes (208.3F/g) are lower than that of Pickling-SE electrodes (291.5 F/g) at 1A/g. GCDs of various Current density in 1 M Li_2SO_4 electrolyte are presented in Figure 8c and 8d, respectively. The charge-discharge curve exhibits an approximately symmetrical shape with a quasi-linear slope at all current densities, resulting in high charge-discharge coulombic efficiency and low polarization of the three electrodes. The nonlinearity of the potential-time curve becomes sharper as the current density decreases. This is a characteristic pseudo-constant charge/discharge process on the entire potential window. Compared to the NaOH electrolyte, the potential window extends downward about 1.4V in Li_2SO_4 electrolyte, due to the neutral nature and passivated capability of Li_2SO_4 electrolyte [37].

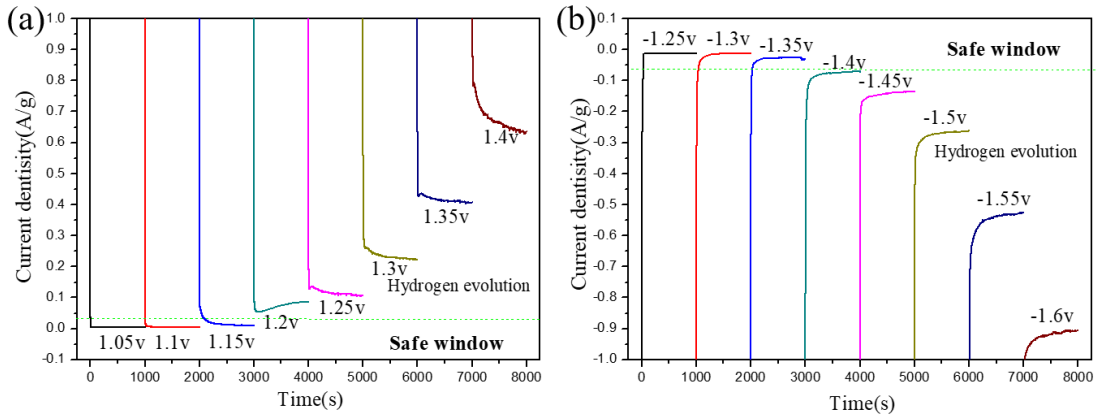

Figure 9. Chronoamperometry data collected at different potentials for Pickling-SE electrodes in 1M Li_2SO_4.

Based on the observed current density values (Figure 7a), we divide the potential of CA into two schemes: (i) the "safe" region (marked green), and the current density does not exceed ≈0.05A/g (Show in Figures 9a and 9c) and no H_2 evolution, and (ii) H_2 - evolutionary regions were observed, where current densities > 0.05 A/g and active H_2 release were observed. The onset of hydrogen evolution (start of Scheme 2) limits the cathode potential of the electrode used. It is worth noting that this method of selecting voltage windows and estimating the contribution of various parasitic reactions is also applicable to other supercapacitor materials/devices. In this case, it allows us to estimate the extent of H_2 evolution by simply measuring current transients, where H_2 bubble formation is reflected by the non-uniform current distribution. Therefore, the minimum negative voltage and "safe" voltage limit for the pickled SE electrode in 1M Li_2SO_4 relative to Ag/AgCl is -1.3V to 1.1V. As mentioned above, one of the underlying mechanisms of high capacitance is electrochemical hydrogen storage, as already indicated for some carbon materials.

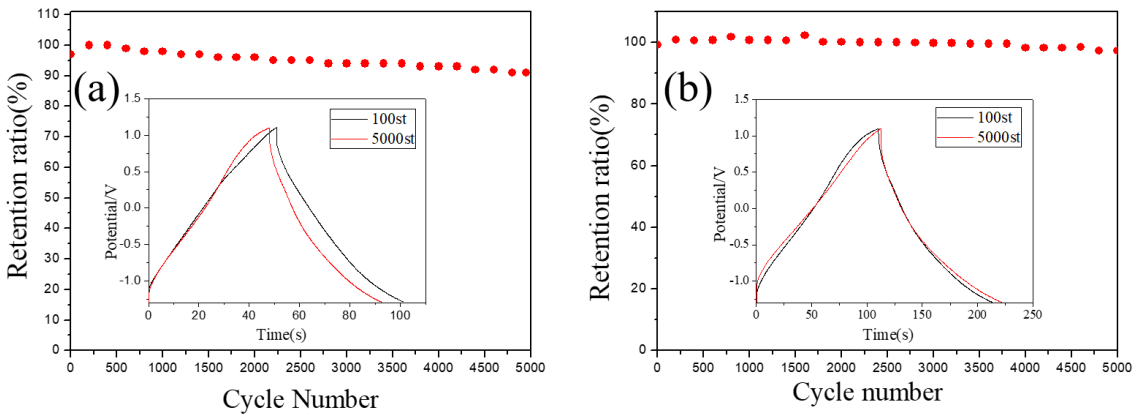

Figure 10. Cycling performance of Original-SE electrodes (a) and Pickling-SE electrodes (b) 1M Li_2SO_4 electrolyte of 5.0 A g^{-1} (inset: the charge–discharge curves of the 100st and 5000th cycle).

Furthermore, the long-term cyclic stability of the Original-SE electrodes and Pickling-SE electrodes are investigated using galvanostatic charge–discharge measurement at a current density of 5 A g^{-1} within a potential window of -1.3–1.1 V (vs. Ag/AgCl). As shown in 1st to100th cycle, the retention ratio seems to have occurred a small increase, that might be an activation diffusion process, and the retention ratio reaches steady state eventually. The long term performance maintains at about 97.2% of the Pickling-SE electrodes (Figure 10b) over 5000 cycles, which shows a more excellent stability than that 91.1% of Original-SE electrode (Figure 10a). This variation may be due to the effects from richer porosity of the electrode to expose additional surface area and easier for electrolyte ions transport. Additionally, the 100st and 5000th cycle galvanostatic charge–discharge curve (inset in Figure 10a and Figure 10b) still displayed a symmetrical triangular shape, indicating that the fexible supercapacitor possesses stable electrochemical performance and good charge propagation. All the data above indicate that the Pickling-SE electrode is more suitable for supercapacitors than the Original-SE electrode.

Table 1. A summary of the electrode materials and their corresponding specific capacitances

Composition	Specific capacitance and current density	Ref.
Coconut shell derived microporous carbon for supercapacitors	150.0 F g^{-1} with 1A g^{-1}	[38]
Grape seed composite graphene oxide for supercapacitors	260.0F g^{-1} with 1A g^{-1}	[39]
Onion as a precursor to obtain lignin - potassium salt / cellulose composite for supercapacitors	179.5F g^{-1} with 1A g^{-1}	[40]
High-surface area carbons are produced from biomass-based products (wood sawdust and tannic acid) for supercapacitors	200.0 F g^{-1} with 1A g^{-1}	[41]
the preparation of partially graphitic nanoporous carbon	173.2 F g^{-1} with 1A g^{-1}	[42]

from biomass (bamboo bagasse) for supercapacitors		
Pickling silkworm material for supercapacitors in this work	291.5 F g^{-1} with 1A g^{-1}	This work
Original silkworm material for supercapacitors in this work	208.3 F g^{-1} with 1A g^{-1}	This work

The comparison of the specific capacitances performance of the silkworm electrode materials with other electrode materials reported in literatures for the application of supercapacitor was shown in Table 1. The results in this table showed that silkworm electrode exhibits higher capacity than other electrodes, indicating Pickling-SE material own very good the electrochemical performance and capacity.

4. CONCLUSION

In summary, mesoporous carbon derived from biomass materials of silkworm excrement as the precursors via chemical pickling process. The electrochemical performance of the electrodes were characterized. electrochemical measurements have been demonstrated that the obtained Pickling-SE electrode shows higher specific capacitance and cycle stability than Original-SE Introduction. electrochemical performance of a specific capacitance of 291.5 F/g for Pickling-SE electrodes than that 208.3 F/g for Original-SE electrodes at 1A/g in 1M Li_2SO_4 electrolyte, and a higher stability for Pickling-SE electrodes (97.2%) than Original-SE electrodes (91.1%) over 5000 cycles. This high supercapacitor performance can be attributed to both of the specific capacitance and capacitive retention increase with the increase of the surface area and fraction of the mesopores.

References

1. R.H. Cherry, *Bulletin of the ESA.*, 33(1987)83.
2. H.J. Kim, K.Y. Kim, S.D. Ji and H.T. Lee, *J. Asia-Pac. Entomol.*, 20(2017) 1001.
3. R.G. Wang, J.K. Guo, Y.M. Xu, Y.Z. Ding, Y. Shen, X.Q. Zheng and R.W. Feng, *Ecotoxicol. Environ. Saf.,* 124 (2016) 239.
4. Y.N. Wer, Y.X. Wu, Q. Chang, M.X. Xie, X.H. Wang, J.W. Mo, X.K. He, Z.X. Zhao and Z.X. Zhao, *RSC Adv.*, 7 (2017) 30020.
5. Y.N. Yang, L.M. Tang, L. Tong, Y. Liu, H. Liu and X.M. Li, *Adv. Space. Res.*, 46 (2010) 707.
6. J. Han, Y. Wang, J.J. Ma, Y.C. Wu, Y.T. Hu, L. Ni and Y.F. Li, *Sep. Purif. Technol.*, 115 (2013) 51.
7. G.M.S. ElShafei, I.M.A. ElSherbiny, A.S. Darwish and C.A. Philip, *Chem. Eng. Sci.,* 92 (2014) 461.
8. V. Sahu, S. Grover, B. Tulachan, M. Sharma, G. Srivastava, M. Roy, M. Saxena. N. Sethy, K. Bhargava, D. Philip, H. Kim, G. Singh, S.K. Singh, M. Das and R.K. Sharma, *Electrochim. Acta.*, 160 (2015) 244.
9. L. Tong, D. Hu, L. Hong, M. Ling, Y. Fu, B. Jia, F. Du and E. Hu, *Ecol. Eng., 37 (2011) 2025.*
10. L. Tong, D.W. Hu, Y.M. Fu, B.Z. Xie and H. Liu, *Ecol. Eng.*, 47 (2012) 105.
11. S.R. Chen, J.Y. Liang, J.X. Zhao, H.F. Li, Y. Liu, H.M. Deng, C. Liu, S. Tang and Y.C. Cao, Chin.

Chem. Lett., 30 (2019) 787.
12. Q.Y. Sun, T.Y. Jiang, G.Z. Zhao and J.Y. Shi, *Int. J. Electrochem. Sci*., 14 (2019) 1.
13. C.F. Liu, Y.C. Liu, T.Y. Yi and C.C. Hu, *Carbon*., 145 (2019) 529.
14. R.D. Mckerracher, A. Holland, A. Cruden and R.G.A. Wills, *Carbon.*, 144 (2019) 333.
15. M.Li and B.Y. Mu, *Appl. Energ*., 242 (2019) 695.
16. L.J. Hou, Z.A. Hu, X.T. Wang, L.L. Qiang, Y. Zhou, L.W. Lv and S.S. Li, *J. Colloid Interface Sci*., 540 (2019) 88.
17. G.X. Zhang, Y.M. Chen, Y.G. Chen and H.B. Guo, *Mater. Res. Bull*., 102 (2018) 391.
18. Y. Liu, M.Y. Zhang, L.Q. Wang, Y.J. Hou, C.X. Guo, H.Y. Xin and S. Xu, *Chin. Chem. Lett.,* 4 (2019) 5013.
19. M. Yu, Y.Y. Han, Y. Li, J. Li and L.J. Wang, *Carbohydr. Polym*., 199 (2018) 555.
20. S. Cao, J.X. Yang, J. Li, K. Shi and X.K. Li, *Diamond Relat. Mater*., 96 (2019) 118.
21. W.M. Du, Z.R. Zhang, L.G. Du, X.Y. Fan, Z.W. Shen, X.R. Ren, Y.P. Zhao, C.Z. Wei and S.H. Wei, *J. Alloys Compd*., 797 (2019) 1031.
22. B. Wang, L.L. Ji, Y.L. Yu, N.X. Wang, J. Wang and J.B. Zhao, *Electrochim. Acta*., 309 (2019) 39.
23. W. Gou, B. Xie, C. Xu, Z. Zheng, J. J. He, Dan, Huang and N. Geng, *Int. J. Electrochem. Sci*., 14 (2019) 494.
24. E. Azwer, W.A.A. Mahair, J.H. Chuah, D.V..N. Vo, N.L. Ma, W.H. Lam and S.S. Lam, *Int. J. Hydrogen Energy*., 43 (2018) 20811.
25. F.Q. Guo, X.C. Jiang, X.P. Jia, S. Liang, L, Qian and Z.H. Rao, *J. Electroanal. Chem*., 844 (2019) 105.
26. B.B. Krishna, B. Biswas, P. Ohri, J. Kuman, R. Singh and T. Bhashar, *Renew Energ.*, 98 (2016) 238.
27. S. Herou, P. Schlee, A.B. Jorge and M. Titirici, *Green Chem*., 9 (2018) 18.
28. C. Wang, Y. Xiong, H.W. Wang and Q.F. Sun, *J. Colloid Interface Sci.J.,* 528 (2018) 349.
29. Y. Hou and J.G. Jiang, *Food Funct*., 4 (2013) 1727.
30. L. Chen, Y.Z. Zuo, Y. Zhang and Y.M. Gao, *Int. J. Electrochem. Sci.,* 13 (2018) 642.
31. H.X. Liang, B. Song, P. Peng, G.J. Jiao, X. Yan and D. She, *Chem. Eng. J.,* 367 (2019) 9.
32. X.Y. Fu, L. Liu, Y.F. Yu, H.J. Lv, Y. Zhang, S.L. Hou and A.B. Chen, J. TaiWan. *Inst. Chem. E*., 101 (2019) 244.
33. P.T. Liu, Y.Y. Wang and J.H. Liu, *J. Energy. Chem*., 34 (201) 171.
34. C.N.S. Kumar, V.S.K. Chakravadhanula, A. Riaz, S. Dehm, D. Wang, X.K. Mu, B. Flavel, R. Krupke and C. Kubel, *Nanoscale.*, 23 (2017) 1722.
35. Y.H. Cao, K.L. Wang, X.M. Wang, Z.G. Gu, Q.H. Fan, W. Gibbons, J.D. Hoefelmeyer, P.R. Kharel and M. Shrestha, *Electrochim. Acta.*, 212 (2016) 839.
36. K. Mukdasai and S. Mukdasai, *Int. J. Electrochem. Sci.,* 13 (2018) 58.
37. Y.H. Wang, X.Q. Cui, Y.Y. Zhang, L.J. Zhang, X.G. Gong, and G.F. Zheng, *Adv. Mater.,* 28 (2016) 7626.
38. E. Redondo, J.L. Segalini, J.C. Gonzalez, E. Goikolea and R. Mysyk, *Electrochim. Acta*., 293 (2019) 49
39. L. Guardia, L. Suarez, N. Querejata, V. Vretenar, P. Kotrusz, V. Skakalova and T.A. Centeno, *Electrochim. Acta*., 298 (2019) 910.
40. W.L. Zhang, J.H. Xu, D.X. Hou, J. Yin, D.B. Liu, Y.P. He and H.B. Lin, *J. Colloid Interface Sci*.,530 (2018) 338.
41. M. Sevilla, N. Diez, G.A. Ferrero and A.B. Fuertes, *Energy Storage Mater.,* 18 (2019) 356.
42. S.S. Gunasekaran, S.K. Elumalali, T.K. Kumaresan, R. Meganathan, A. Ashok, V. Pawar, K. Vediappan, G. Ramasamy, S.Z. Karazhanov, K. Raman and R.S. Bose, *Mater. Lett.,* 218 (2018) 165.